Spontaneous emission in leaky modes of nanowires

© *V.V. Nikolaev*[1], *E.I. Girshova*[1,¶], *M.A. Kaliteevski*[2]

[1] Ioffe Institute,
194021 St. Petersburg, Russia
[2] ITMO University,
197021 St. Petersburg, Russia

[¶] E-mail: ilinishna@gmail.com

Analytical expressions for spontaneous emission pro-bability in the vicinity of nanowire for the emitter oriented in axial, radial and azimuthal direction in respect to the nanowire axis, has been obtained. Directionality of emission and probability of emission have been calculated for various positions of emitter. Enhancement of the spontaneous emission probability by one order of magnitude, and formation of the sharp directionality diagram has been demonstrated.

Keywords: nanowire, spontaneous emission, leaky modes.

1. Introduction

Progress in nanowire growth technology made it possible to fabricate various optoelectronic devices based on them, in particular LEDs [1,2], sensors [3,4] and single photon sources [5–7]. The technology of creating nanowires makes it possible to create structures with a variable profile of the chemical composition and morphological structure of the material depending on the radius and position along the axis [8–10]. The nanowire is a spatial heterogeneity of the permittivity, which can lead to a change in the probability of spontaneous emission (Purcell effect) for an emitter located inside the nanowire or outside it [11,12].

There are many works related to the calculation of the probability of spontaneous emission for nanowires using different theoretical formalism. The method based on the Green's functions of the electromagnetic field for heterogeneous structures uses a cumbersome formalism and does not allow one to obtain the final expressions for the probability of spontaneous emission in a certain direction in the form of an algebraic expression [13–15]. The formalism based on the used concept of the local density of states [16] is inconvenient to analyze the influence of the spatial orientation of the emitter on the probability of spontaneous emission, since in the case of spatially heterogeneous structures the small energy range may contain modes with different electric field directions in the point where the emitter is located, which can be especially pronounced in the case of optical resonance. A significant part of the studies related to calculation of the probability of spontaneous emission uses numerical methods, the results of which, obviously, have limited applicability from the point of view of describing the physical nature of this or that phenomenon. Despite a significant number of studies on this topic, algebraic expressions for the probability of spontaneous

emission in a fixed direction for a certain orientation of the emitter located inside or near the dielectric cylinder were not yet obtained. This circumstance significantly complicates the analysis of emission processes in nanowires, as well as the creation of devices based on them.

Besides, analysis of emission processes in nanowire sometimes is limited by describing the interaction of the emitter with waveguide modes, ignoring emission into free space (leaking modes), which is possibly due to the presence of a fundamental waveguide mode HE11, which exists at any value of the radius of a cylindrical waveguide. It should be taken into account that at small waveguide radius the probability of emission into the wave mode is very small [17–21], and the main contribution to the emission is made by leaking modes.

The purpose of this paper is to obtain algebraic expressions for the probability of spontaneous emission into leaking modes for the emitter oriented radially, axially, or azimuthally with respect to the nanowire axis, depending on the position of the emitter and direction of emission, as well as the calculation of the Purcell coefficient, and directional radiation pattern.

The structure scheme is shown in Fig. 1: the emitter can be oriented axially (along the axis of the nanowire z), radially (perpendicular to the axis z), or azimuthally. The refraction indices of the nanowire and the environment are 3.5 and 1.0, respectively.

2. Main equations

2.1. Scattering matrix of cylindrical electromagnetic waves

Let us consider a homogeneous medium characterized by dielectric and magnetic permeabilities ε_1 and μ_1 respectively, in which a cylinder of radius ρ_0 and with
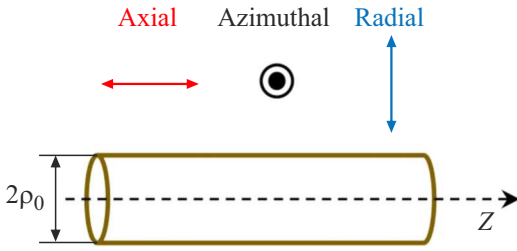
Figure 1. Structure diagram: nanowire and possible dipole orientations.

permeabilities ε_2 and μ_2 is placed. For this system, we introduce a cylindrical coordinate system $\{\rho, \phi, z\}$, where the axis z is directed along the symmetry axis of the nanowire.

Consider a monochromatic electromagnetic field of cyclic frequency ω with a fixed wavenumber k_z. The electric and magnetic components of the field will be proportional to the factor $\exp(ik_z z)\exp(-i\omega t)$. If the wavenumber k_z is less than the wave vector of light in the external medium $\sqrt{\varepsilon_1\mu_1}k_0$, where $k_0 = \omega/c$ is the wave vector in vacuum, then the field under consideration will consist of electromagnetic waves propagating at an angle to the structure axis, at that $\cos(\theta) = k_z/(\sqrt{\varepsilon_1\mu_1}k_0)$. In a homogeneous medium such electromagnetic field can be represented as a sum

$$\mathbf{E}_{k_z}(\mathbf{r}) = \sum_{m=-\infty}^{+\infty} \sum_{\substack{J=\text{TM,TE} \\ i=1,2}} A_{J,m}^{(i)} \tilde{\mathbf{E}}_{J,m}^{(i)}(\rho) \exp(im\phi) \exp(ik_z z),$$

(1)

where the summation occurs over integer values of the quantum number of the azimuthal angular momentum m. Index J denotes TM- (transverse magnetic) or TE- (transverse electric) polarization (the common time factor is omitted hereinafter). Index $i = 1, 2$ denotes divergent and convergent cylindrical waves, respectively. The dimensionless electric field profiles $\tilde{\mathbf{E}}_{J,m}^{(i)}(\rho)$ are related to vector cylindrical harmonics [22]:

$$\tilde{\mathbf{E}}_{\text{TM},m}^{(i)}(\rho) = \frac{1}{k_\rho} \mathbf{N}_m^{(i)}(\rho),$$

(2a)

$$\tilde{\mathbf{E}}_{\text{TE},m}^{(i)}(\rho) = \frac{1}{k_\rho} \mathbf{M}_m^{(i)}(\rho),$$

(2b)

where $k_\rho = \sqrt{\varepsilon\mu k_0^2 - k_z^2}$ is the transverse component of the wave vector, which in the general case can be complex. The dimensionless magnetic field profiles corresponding to the electric fields in (2) have the form (in this paper we use the Gaussian system of units):

$$\tilde{\mathbf{H}}_{\text{TM},m}^{(i)}(\rho) = -\sqrt{\frac{\varepsilon}{\mu}} \tilde{\mathbf{E}}_{\text{TE},m}^{(i)}(\rho) = -\sqrt{\frac{\varepsilon}{\mu}} \frac{i}{k_\rho} \mathbf{M}_m^{(i)}(\rho), \quad (3a)$$

$$\tilde{\mathbf{H}}_{\text{TE},m}^{(i)}(\rho) = -\sqrt{\frac{\varepsilon}{\mu}} \tilde{\mathbf{E}}_{\text{TM},m}^{(i)}(\rho) = -\sqrt{\frac{\varepsilon}{\mu}} \frac{i}{k_\rho} \mathbf{N}_m^{(i)}(\rho). \quad (3b)$$

Vector cylindrical harmonics are given by the following expressions [18,19]:

$$\mathbf{N}_m^{(i)}(\rho) = \frac{1}{\sqrt{\varepsilon\mu}} \frac{k_\rho}{k_0} \left(ik_z H_m'^{(i)}(k_\rho\rho)\mathbf{e}_\rho \right.$$

$$\left. - mk_z \frac{H_m^{(i)}(k_\rho\rho)}{k_\rho\rho} \mathbf{e}_\phi + k_\rho H_m^{(i)}(k_\rho\rho)\mathbf{e}_z \right), \quad (4a)$$

$$\mathbf{M}_m^{(i)}(\rho) = k_\rho \left(im \frac{H_m^{(i)}(k_\rho\rho)}{k_\rho\rho} \mathbf{e}_\phi - H_m'^{(i)}(k_\rho\rho)\mathbf{e}_\phi \right), \quad (4b)$$

where we selected the Hankel functions of the first and second kind $H_m^{(1)}(x)$ and $H_m^{(2)}(x)$ as linearly independent solutions of the Bessel equation; the derivative in the Hankel functions, where present, is taken over the entire argument. This choice is convenient for representing converging (given by the function $H_m^{(2)}$) and diverging ($H_m^{(1)}$) cylindrical waves. Equations (2)−(4) show that TM(TE)-polarized fields have a zero magnetic (electric) field component along the symmetry axis of the structure. The constant coefficients $A_{\text{TM/TE},m}^{(1/2)}$ in (1) define a particular type of field. Thus, a plane linearly polarized wave propagating along the positive direction of the axis x at an angle to the axis z will be given by the coefficients $A_{\text{TM},m}^{(1)} = A_{\text{TM},m}^{(2)} = i^m E_0/2$, $A_{\text{TE},m}^{(1)} = A_{\text{TE},m}^{(2)} = 0$ for the case of a magnetic field perpendicular to the axis z (TM-polarization), and $A_{\text{TE},m}^{(1)} = A_{\text{TE},m}^{(2)} = i^m E_0/2$, $A_{\text{TM},m}^{(1)} = A_{\text{TM},m}^{(2)} = 0$ for TE-polarization when the electric field is perpendicular to the axis z. Here E_0 is the amplitude of the electric field of the plane wave. The expansion of the field of the form (1) can be applied both for the external medium and for the cylinder, despite the fact that inside the cylinder instead of the Hankel functions it is more convenient to use the Bessel function $J_m(x)$, which does not diverge on the axis of symmetry.

The center of our formalism contains the scattering matrix $\hat{s}_m$ of the cylinder for cylindrical waves with fixed angular moment m and wavenumber k_z:

$$\begin{pmatrix} A_{\text{TM},m}^{(1)} \\ A_{\text{TE},m}^{(1)} \end{pmatrix} = \hat{s}_m(k_z) \begin{pmatrix} A_{\text{TM},m}^{(2)} \\ A_{\text{TE},m}^{(2)} \end{pmatrix}. \quad (5)$$

The scattering matrix in expression (5) relates the amplitude coefficients $A_{\text{TM/TE},m}^{(2)}$ for converging cylindrical waves with the corresponding coefficients $A_{\text{TM/TE},m}^{(1)}$ of waves reflected from the cylinder. Analytic expressions for this matrix are derived from the continuity condition for the tangential components of the electric $\mathbf{E}$ and magnetic $\mathbf{H}$ fields at the cylinder boundary:

$$\hat{s}_m(k_z) = -\frac{H_m^{(2)}(\tilde{k}_{\rho 1})}{H_m^{(1)}(\tilde{k}_{\rho 1})} \frac{1}{T_{\varepsilon,m}^{(1)}T_{\mu,m}^{(1)} - m^2 U^2}$$

$$\times \begin{pmatrix} T_{\varepsilon,m}^{(2)}T_{\mu,m}^{(1)} - m^2 U^2 & -V_m \\ V_m & T_{\varepsilon,m}^{(1)}T_{\mu,m}^{(2)} - m^2 U^2 \end{pmatrix}, \quad (6)$$

where

$$T_{\varepsilon,m}^{(i)} = \tilde{H}_m^{(i)}(\tilde{k}_{\rho 1}) - \frac{\varepsilon_2}{\varepsilon_1}\tilde{J}_m(\tilde{k}_{\rho 2}),$$

$$T_{\mu,m}^{(i)} = \tilde{H}_m^{(i)}(\tilde{k}_{\rho 1}) - \frac{\mu_2}{\mu_1}\tilde{J}_m(\tilde{k}_{\rho 2}),$$

$$U = \frac{1}{\sqrt{\varepsilon_1\mu_1}}\frac{k_z}{k_0}\left(\frac{1}{\tilde{k}_{\rho 1}^2} - \frac{1}{\tilde{k}_{\rho 2}^2}\right),$$

and

$$V_m = m\frac{4}{\pi}\frac{1}{\tilde{k}_{\rho 1}^2}\frac{U}{H_m^{(1)}(\tilde{k}_{\rho 1})H_m^{(2)}(\tilde{k}_{\rho 1})}.$$

Here

$$\tilde{k}_{\rho 1/2} = \rho_0\sqrt{\varepsilon_{1/2}\mu_{1/2}\,k_0^2 - k_z^2}$$

there are dimensionless transverse components of the wave vector in the external medium and inside the cylinder, which in the general case can be complex. Also the following notations are introduced

$$\tilde{H}_m^{(i)}(x) = H_m'^{(i)}(x)/\left(xH_m^{(i)}(x)\right)$$

and

$$\tilde{J}_m(x) = J_m'(x)/\left(x\,J_m(x)\right).$$

Expression (6) is valid for any value k_z and any complex optical parameters of the external medium and the cylinder. For the metallic material of the cylinder it may be convenient to express

$$\tilde{J}_m(x) = -I_m'(-ix)/\left(-ix\,I_m(-ix)\right) = -\tilde{I}_m(-ix),$$

where I_m is the modified Bessel function.

In a more compact form the scattering matrix can be written as

$$\hat{s}_m(k_z) = -\frac{H_m^{(2)}(\tilde{k}_{\rho 1})}{H_m^{(1)}(\tilde{k}_{\rho 1})}\frac{1}{\theta_{Disp,m}}\begin{pmatrix}\theta_{TM,m} & -V_m \\ V_m & \theta_{TE,m}\end{pmatrix}, \qquad (7)$$

where

$$\theta_{Disp,m} = T_{\varepsilon,m}^{(1)}T_{\mu,m}^{(1)} - m^2U^2, \quad \theta_{TM,m} = T_{\varepsilon,m}^{(2)}T_{\mu,m}^{(1)} - m^2U^2$$

and

$$\theta_{TE,m} = T_{\varepsilon,m}^{(1)}T_{\mu,m}^{(2)} - m^2U^2.$$

The elements of the scattering matrix (6), (7) are related to the scattering coefficients Mi for the cylinder [22]:

$$\hat{s}_m = -2\begin{pmatrix}b_{mI} - \frac{1}{2} & b_{mII} \\ a_{mI} & a_{mII} - \frac{1}{2}\end{pmatrix}, \qquad (8)$$

where the Mi coefficients can be used to calculate the scattering cross-section of the cylinder for the plane wave TE-polarization [15]:

$$\sigma = \frac{2}{k_0\rho_0}\left(|a_{0II}|^2 + 2\sum_{m=1}^{+\infty}|a_{mII}|^2 + |b_{mII}|^2\right). \qquad (9)$$

To calculate the scattering cross-section of TM-polarized plane wave, it is necessary to replace $\{a_{mII}, b_{mII}\}$ in (9) with the coefficients $\{b_{mI}, a_{mI}\}$. In (9) the scattering cross-section is reduced to the length of the cylinder.

2.2. Emission to outer space

To calculate the rate of spontaneous recombination into the outer space using the golden Fermi rule, it is necessary to specify the procedure for quantizing modes capable of transferring emission energy outside the structure. Let us consider a quantization cylinder of radius R, which we subsequently tend to infinity. By analogy with (6), one can obtain the expression for the scattering matrix for the entire quantization cylinder $\hat{S}$. In the limit of large radius R this matrix has the form

$$\hat{S}_m(k_z) = \exp\left(i\left[2k_{\rho 1}\rho_0 - m\pi - \frac{\pi}{2}\right]\right)\hat{\tilde{s}}_m(k_z), \qquad (10)$$

where $\hat{\tilde{s}}_m$ is the modified scattering matrix of the cylinder, which differs from $\hat{s}_m$ by multiplying with -1 of the elements of the second row ($\hat{s}_m[2,1]$ and $\hat{s}_m[2,2]$).

As a quantization condition, we equate to zero the tangential components of the field on the surface of the quantization cylinder. From a qualitative point of view, this condition resembles the quantization of electron-hole pairs in a continuous spectrum (Eliott's formula). In terms of the scattering matrix, the quantization condition comes down to the following:

1) at quantized frequencies the eigenvalues of the matrix $\hat{S}_m$ are -1;

2) electromagnetic fields of quantized modes correspond to the eigenvectors of the modified scattering matrix of the cylinder $\hat{\tilde{s}}_m$.

The first item is the condition for the phase in the exponent in equation (10) and leads to quantization of the transverse wave vector $k_{\rho 1}$ in the external medium. Adding to this the Born−Karman condition along the axis of the cylinder, which gives the quantization of the longitudinal vector k_z, as well as the normalization of the electromagnetic field to the photon energy inside the quantization cylinder, and tending R to infinity, one can obtain the spectrum of electromagnetic field eigenmodes.

The expression for the probability of spontaneous emission for a transition between two quantum states has the form

$$W = \frac{2\pi}{\hbar}|\mathbf{d}_{fi}|^2\sum_P|\mathbf{E}_P(\mathbf{r}_0)\mathbf{e}_d|^2\delta(\hbar\omega_{fi} - \hbar\omega_P), \qquad (11)$$

where $|\mathbf{d}_{fi}|$ is the matrix element of the optical transition dipole moment, $\hbar\omega_{fi}$ is the optical transition energy, $\hbar\omega_P$ is the photon energy of the quantized normalized optical mode and is the complex amplitude of the electric field at the point where the emitter is located. The summation occurs over all possible quantized modes (characterized by the index P); the specific form of these modes depends on the used quantization rules. The summation over all modes with index P is the summation over azimuth numbers m, polarizations J, and also over modes quantized in z and ρ directions:

$$\sum_P \to \sum_m\sum_{J=EH,HE}\sum_{N_z}\sum_{N_\rho}, \qquad (12)$$

which can be converted to form

$$\sum_P \to \sum_m \sum_{J=\text{EH,HE}} \varepsilon_1 \mu_1 \frac{R L_z}{\pi 2} \int \frac{\hbar \omega_P}{(\hbar c)^2} \, d\theta d(\hbar \omega_P). \quad (13)$$

The rate of spontaneous recombination into leaking modes can be written as

$$W_{\text{rad}} = \frac{3}{16} W_1 \sum_{m=-\infty}^{+\infty} \sum_{J=\text{EH,HE}} \int_0^\pi |\tilde{\mathbf{E}}_m^J(\rho) \mathbf{e}_d|^2 \sin\theta d\theta, \quad (14)$$

where

$$W_1 = \frac{4}{3} \mu_1 \sqrt{\varepsilon_1 \mu_1} \frac{k_0^3}{\hbar} |\mathbf{d}_{fi}|^2$$

— total recombination rate in external homogeneous medium and $\mathbf{d}_{fi} = |\mathbf{d}_{fi}| \mathbf{e}_d$ — matrix element of the dipole moment of the optical transition. The corresponding unit complex vector $\mathbf{e}_d$ specifies the polarization of the optical transition. The expression $\tilde{\mathbf{E}}_m^J(\rho)$ is the normalized dimensionless field profile corresponding to the eigenmodes of the quantization cylinder with ideally conducting cylindrical walls, or, which is the same, to the eigenvectors of the modified scattering matrix $\hat{\tilde{s}}_m$. The index $J = \text{EH, HE}$ marks the polarization of the mode, which in turn corresponds to one of the two eigenvectors of the modified scattering matrix (see below). The dimensionless profile of the electric field in the external medium has the form

$$\tilde{\mathbf{E}}_m^J(\rho) = \sum_{i=1,2} \tilde{A}_{\text{TM},m}^{J,(i)} \tilde{\mathbf{E}}_{\text{TM},m}^{(i)}(\rho) + \tilde{A}_{\text{TE},m}^{J,(i)} \tilde{\mathbf{E}}_{\text{TE},m}^{(i)}(\rho), \quad (15)$$

where TM and TE are polarized field profiles $\tilde{\mathbf{E}}_{\text{TM/TE},m}^{(i)}(\rho)$ are given in (2), (4). Pairs of dimensionless coefficients for convergent cylindrical waves $\{\tilde{A}_{\text{TM},m}^{\text{EH},(2)}, \tilde{A}_{\text{TE},m}^{\text{EH},(2)}\}$ and $\{\tilde{A}_{\text{TM},m}^{\text{HE},(2)}, \tilde{A}_{\text{TE},m}^{\text{HE},(2)}\}$ are eigenvectors of the matrix $\hat{\tilde{s}}_m$. Corresponding coefficients for divergent waves $\{\tilde{A}_{\text{TM},m}^{\text{EH/HE},(1)}, \tilde{A}_{\text{TE},m}^{\text{EH/HE},(1)}\}$ are obtained using (5). Normalizing the eigenmodes of the quantization cylinder in this context means the following equalities: $|\tilde{A}_{\text{TM},m}^{J,(2)}| + |\tilde{A}_{\text{TE},m}^{J,(2)}| = 1$ for the polarization index $J = \text{EH, HE}$ and similarly for the coefficients for divergent waves. Such a normalization (as well as similar quantization rules in general) is possible if the absorption in the cylinder and the external medium is negligibly small (the optical constants of the cylinder medium can be considered real). In this case, the quantities $\theta_{\text{TM},m}$ and $\theta_{\text{TE},m}$, which determine the diagonal elements of the scattering matrix, are the complex conjugate $\theta_{\text{TE},m} = (\theta_{\text{TM},m})^*$, and the value V_m defining the diagonal elements is real.

The normalized eigenvectors of the modified scattering matrix can be chosen in the following form:

$$\tilde{A}_{\text{TM},m}^{\text{EH},(2)} = \tilde{A}_{\text{TE},m}^{\text{HE},(2)} = \frac{X_{R,m}}{\sqrt{X_{R,m}^2 + V_m^2}}, \quad (16a)$$

$$\tilde{A}_{\text{TE},m}^{\text{EH},(2)} = -\tilde{A}_{\text{TM},m}^{\text{HE},(2)} = -\frac{V_m}{\sqrt{X_{R,m}^2 + V_m^2}}, \quad (16b)$$

where

$$X_{R,m} = \text{Re}\{\theta_{\text{TM},m}\} + \sigma \sqrt{\text{Re}\{\theta_{\text{TM},m}\})^2 + V_m^2},$$

and the constant $\sigma = \text{sign}(\text{Re}\{\theta_{\text{TM}}(k_z = 0)\})$ is determined by the sign of the value $\text{Re}\{\theta_{\text{TM}}\}$ for angle of propagation perpendicular to the structure axis.

Using the eigenvalues of the modified scattering matrix $\tilde{\beta}^\pm$

$$\tilde{\beta}^\pm = \left\{ -\frac{H_m^{(2)}(k_{\rho 1})}{H_m^{(1)}(k_{\rho 1})} \frac{1}{\theta_{Disp,m}} \right\}$$
$$\times \left(i \, \text{Im}\{\theta_{\text{TM},m}\} \pm \sigma \sqrt{(\text{Re}\{\theta_{\text{TM},m}\})^2 + V_m^2} \right) \quad (17a)$$

it is possible to express the coefficients for converging waves in the equation (16):

$$\tilde{A}_{\text{TM},m}^{\text{EH},(1)} = \beta^+ \tilde{A}_{\text{TM},m}^{\text{EH},(2)}, \quad (17b)$$

$$\tilde{A}_{\text{TE},m}^{\text{EH},(1)} = -\beta^+ \tilde{A}_{\text{TE},m}^{\text{EH},(2)}, \quad (17c)$$

$$\tilde{A}_{\text{TM},m}^{\text{HE},(1)} = \beta^- \tilde{A}_{\text{TM},m}^{\text{HE},(2)}, \quad (17d)$$

$$\tilde{A}_{\text{TE},m}^{\text{HE},(1)} = -\beta^- \tilde{A}_{\text{TE},m}^{\text{HE},(2)}. \quad (17e)$$

It can be shown analytically that in the absence of absorption and amplification in the structure, the moduli of the eigenvalues are equal to unity $|\tilde{\beta}^\pm| = 1$. Now we can clarify the division of quantized modes into EH- and HE-polarizations. For perpendicular propagation ($\theta = \pi/2$, $k_z = 0$), the value V_m, which, as can be seen from the expression of the scattering matrix (6), determines the mixing of TM- and TE-polarizations, is equal to zero. In this case, from relations (16), (17) we obtain $\tilde{A}_{\text{TE},m}^{\text{EH},(2)} = \tilde{A}_{\text{TE},m}^{\text{EH},(1)} = 0$, i.e., the quantized mode of EH-type is purely TM-polarized provided there is no mixing of polarizations. Similarly, for perpendicular propagation the HE-mode is TE-polarized. As the angle θ changes, the quantized modes become mixed, and the fractions of TM- and TE-polarizations in them change continuously. Thus, we introduced the notation of quantized modes by analogy with the generally accepted names of waveguide modes, where mixed EH (HE) modes tend to become TM (TE) polarized as mixing tends to zero.

Using the properties of cylindrical vector harmonics (2), (4) when the sign of the azimuthal quantum number m is reversed, the expression (14) for the spontaneous recombination rate can be rewritten as a sum over positive m:

$$\left\{ \frac{3}{16} \right\}^{-1} \frac{W_{\text{rad}}}{W_1} = \int_0^\pi \left(|\tilde{\mathbf{E}}_{m=0}^{\text{TM}}(\rho) \mathbf{e}_{d,p}|^2 + |\tilde{\mathbf{E}}_{m=0}^{\text{TE}}(\rho) \mathbf{e}_{d,s}|^2 \right) \sin\theta d\theta$$
$$+ 2 \sum_{J=\text{EH,HE}} \sum_{m=1}^{+\infty} \int_0^\pi \left(|\tilde{\mathbf{E}}_m^J(\rho) \mathbf{e}_{d,p}|^2 + |\tilde{\mathbf{E}}_m^J(\rho) \mathbf{e}_{d,s}|^2 \right) \sin\theta d\theta.$$
$$(18)$$

Here, the subscript p denotes the part of the emitter polarization vector $\mathbf{e}_d$ lying in the plane containing the axis of the cylinder and the radius vector indicating the emitter position, and the subscript s indicates the remaining part of the vector perpendicular to this plane, $\mathbf{e}_d = \mathbf{e}_{d,p} + \mathbf{e}_{d,s}$. The vector $\mathbf{e}_{d,p}$ can be expressed by the unitary vectors of the cylindrical coordinate system $\mathbf{e}_\rho$ and $\mathbf{e}_z$, while the vector $\mathbf{e}_{d,s}$ contains only the unitary vector $\mathbf{e}_\phi$. Expression (18) takes into account that at $m = 0$ there is no mixing of TM- and TE-polarizations and, thus, the EH mode is TM-polarized, while the HE mode has TE-polarization, and at $m = 0$ TM(TE)-polarized wave interacts only with the part of the optical transition specified by vector $\mathbf{e}_{d,p}(\mathbf{e}_{d,s})$. Thus, the combination of equations (2), (4), (15)−(18) gives analytical expression for the rate of spontaneous recombination of the emitter outside the nanowire.

Expression (18) can be interpreted as decomposition of the spontaneous recombination rate into terms corresponding to emitter emission into modes, each of which is a linear combination of TM- and TE-polarized cylindrical waves with azimuthal numbers of opposite sign $m = \pm|m|$. From expressions (4) for cylindrical waves, one can obtain the angular dependence on the polar coordinate ϕ for the energy flux density of electromagnetic fields formed by various linear combinations of cylindrical waves with $m = \pm|m|$, these dependences are different for TM- and TE-polarized fields. Using this analysis and the obtained expression (18), it is possible to determine what part of the spontaneous emission of the emitter goes into a certain solid angle $do = \sin\theta d\theta d\phi$:

$$\left\{\frac{3}{32\pi}\right\}^{-1}\frac{dW_{\text{rad}}}{W_1 do} = |\tilde{\mathbf{E}}^{\text{TM}}_{m=0}(\rho)\mathbf{e}_{d,p}|^2 + |\tilde{\mathbf{E}}^{\text{TE}}_{m=0}(\rho)\mathbf{e}_{d,s}|^2$$

$$+ 4\sum_{J=\text{EH,HE}}\sum_{m=1}^{+\infty}\Big(|\tilde{\mathbf{E}}^J_m(\rho)\mathbf{e}_{d,p}|^2$$

$$\times \{P^J_{\text{TM},m}\cos^2(m\phi) + P^J_{\text{TE},m}\sin^2(m\phi)\}$$

$$+ |\tilde{\mathbf{E}}^J_m(\rho)\mathbf{e}_{d,s}|^2\{P^J_{\text{TM},m}\sin^2(m\phi) + P^J_{\text{TE},m}\cos^2(m\phi)\}\Big), \tag{19}$$

where the quantities $P^J_{\text{TM/TE},m}$ determine the ratio of TM- and TE-polarizations in the J-polarized mixed quantized mode and are given by the squares of the moduli of the amplitude coefficients (16), (17):

$$P^J_{\text{TM},m} = |\tilde{A}^{J,(1)}_{\text{TM},m}|^2 = |\tilde{A}^{J,(2)}_{\text{TM},m}|^2, \tag{20a}$$

$$P^J_{\text{TE},m} = |\tilde{A}^{J,(1)}_{\text{TE},m}|^2 = |\tilde{A}^{J,(2)}_{\text{TE},m}|^2, \tag{20b}$$

$$P^{\text{EH}}_{\text{TM},m} = P^{\text{HE}}_{\text{TE},m} = \frac{X^2_{R,m}}{X^2_{R,m} + V^2_m}. \tag{20c}$$

When deriving expression (19), it was assumed that the polar coordinate of the emitter is set as $\phi_e = 0$. Expression (19) gives the relative intensity of spontaneous emission into the differential solid angle at large distances from the emitter (in the far field).

3. Results and discussion

The optical properties and spontaneous emission of light in nanowire are determined by the spectrum of its waveguide and leaking modes, while the whispering gallery modes (WGMs) are of decisive importance for the leaking modes.

The values of the reduced radii ρ_0/λ_0, where ρ_0 — the nanowire radius and λ_0 — emission waves in vacuum, for the WGM can be estimated using the relation [23]

$$\rho_0/\lambda_0 = (m + 2j \pm 1/2)/(4n_2), \tag{21}$$

where m — azimuth number, j — „principal quantum number", $n_2 = \sqrt{\varepsilon_2}$ and sign $+(-)$ corresponds to TM(TE) polarization. The exact values of the complex reduced radii are determined for the TM-polarization by the equation

$$n_1 J_m(2\pi n_2\rho_0/\lambda_0)H'^{(1)}_m(2\pi n_1\rho_0/\lambda_0)$$

$$- n_2 J'_m(2\pi n_2\rho_0/\lambda_0)H^{(1)}_m(2\pi n_1\rho_0/\lambda_0) = 0, \tag{22a}$$

where $n_1 = \sqrt{\varepsilon_1}$, and for TE-polarization

$$n_2 J'_m(2\pi n_2\rho_0/\lambda_0)H^{(1)}_m(2\pi n_1\rho_0/\lambda_0)$$

$$- n_1 J_m(2\pi n_1\rho_0/\lambda_0)H'^{(1)}_m(2\pi n_2\rho_0/\lambda_0) = 0. \tag{22b}$$

Note that the WGM with $m = 0$ is sometimes referred to in the literature as an electric dipole (magnetodipole) mode for TM(TE) polarization.

The values of the reduced radii for the azimuthal numbers $m = 0$, 1, 2, 3, 4, 5 are shown in Fig. 2, a. It can be seen that WGM reduced radii, characterized by the values $m = 1$ u 2, have a significant imaginary part; as m increases, the imaginary part rapidly decreases.

Fig. 2, b, c shows the dependence of the Purcell coefficients on the reduced radius of the nanowire for emitter located at the center of the nanowire (b) and at its boundary (c). For axial emitter located at the center of the structure, in the case of a small reduced radius the Purcell coefficient is equal to 1, while for radial emitter the emission is screened.

As the reduced radius increases, peaks of the Purcell coefficient appear, and their position and width are determined by the values of the complex reduced radius for the WGM with $m = 0$ for TM-polarization and $m = 1$ for TE-polarization. This behavior is explained by mode symmetry: at the center of the structure the electric field is nonzero only for TM-modes with $m = 0$ and for TE-modes with $m = 1$. Note that for axial dipole the first peak is observed at a reduced radius of 0.0334, which in practice corresponds to thin nanowires, where emission into the fundamental waveguide mode HE_{11} is suppressed [6]. If the emitter is located at the outer boundary of the cylinder, then the spectrum of the Purcell coefficient changes qualitatively: sharp peaks appear corresponding to whispering gallery modes (WGMs), as shown in Fig. 2, c.
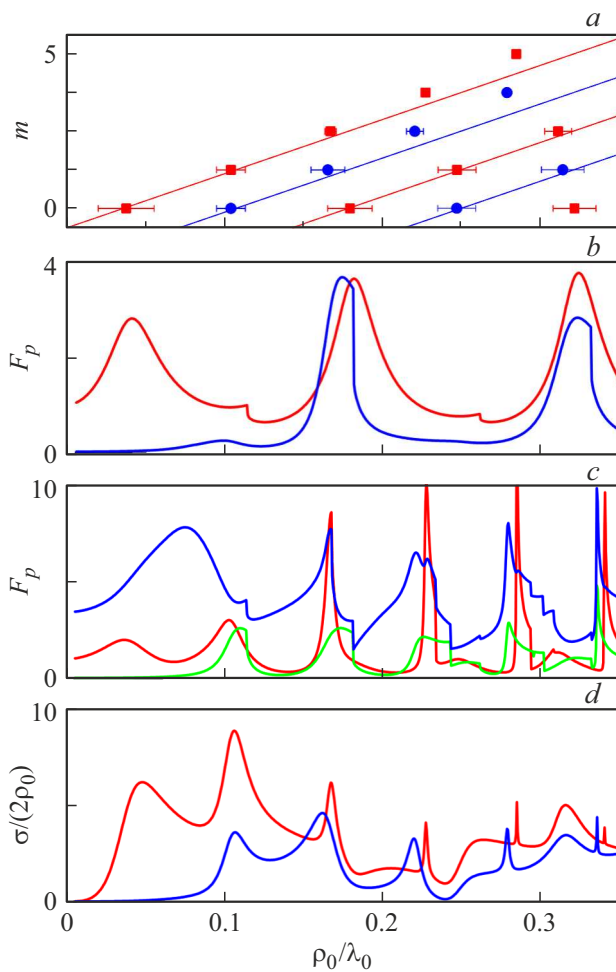
Figure 2. a — nanowire reduced radii corresponding to the WGMs with azimuthal numbers $m = 0, 1, 2, 3, 4$. The imaginary part of the reduced radii is shown as a horizontal line. The solid lines show the estimated dependencies calculated using equation (21). Red squares correspond to TM-modes, blue circles — to TE-modes. (b, c) Purcell coefficient vs. nanowire reduced radius for emitter located on the nanowire axis (b) and on its boundary (c). The red lines correspond to the axial orientation of the dipole, green — azimuthal, blue — radial. d — scattering cross-section of nanowire vs. its reduced radius in the case of TM-polarized (red line) and TE-polarized wave (blue line). (Colored version of the figure is presented in electronic version of the article).

In this case, the peaks corresponding to axial emitters have the highest amplitude; for them, the probability of spontaneous emission increases by an order of magnitude. It can be seen that the peaks corresponding to WGMs are also observed in the scattering efficiency spectra for the TE and TM plane waves shown in Fig 2, c. Dashed vertical lines show the reduced cutoff radii for TM_{01} and TE_{01} ($\rho_0/\lambda_0 = 0.114$) and EH_{11} ($\rho_0/\lambda_0 = 0.181$). For comparison, the dependence of the scattering cross-section of the nanowire is shown (Fig. 2, d). The reduced radii corresponding to WGMs have the following values: TM2 —

0.168, TM3 — 0.228, TE3 — 0.28, TM4 — 0.285, TE4 — 0.336. The refraction indices of the nanowire and the environment are 3.5 and 1.0, respectively.

Fig. 3 shows Purcell coefficient vs. distance from the axis z to the emitter for situations where the reduced radius of the nanowire corresponds to WGMs TM3 (Fig. 3, a), TE3 (Fig. 3, b), TM4 (Fig. 3, c) and TE4 (Fig. 3, d). It can be seen that in the case of TM polarized WGMs, the maximum of the Purcell coefficient takes place inside the nanowire at some distance from the boundary, while in the case of TE polarized modes — at the outer boundary. In all cases considered, the maximum value of the Purcell coefficient for the azimuthal dipole is less than that for the radial and axial dipoles. For TE polarized modes, the emission probability for radial dipole located at the outer boundary of nanowire
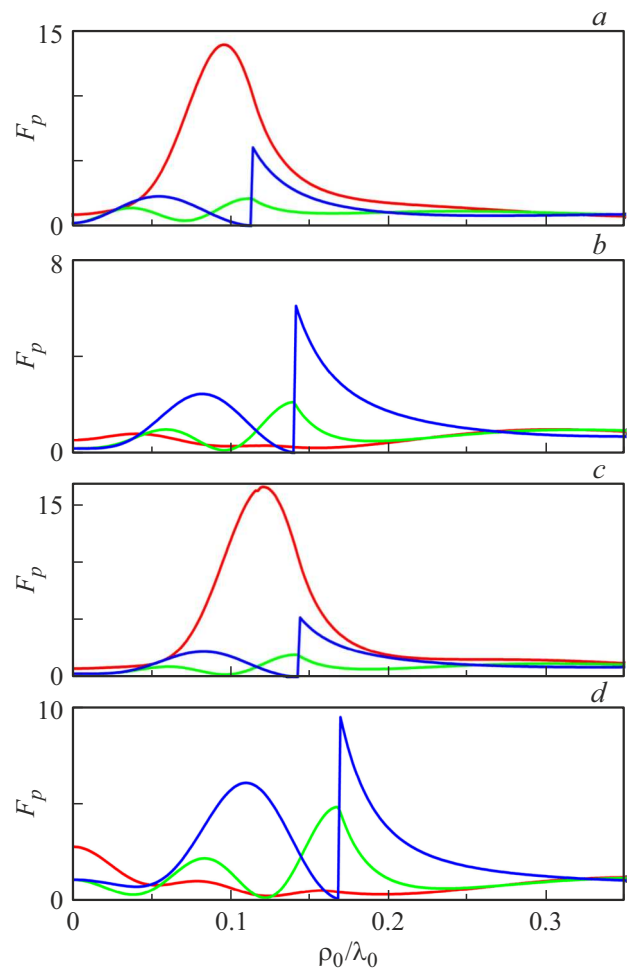
Figure 3. Purcell coefficients vs. position of the emitter for different values of nanowire reduced radius: a — $\rho_0/\lambda_0 = 0.228$, b — $\rho_0/\lambda_0 = 0.28$, c — $\rho_0/\lambda_0 = 0.285$, d — $\rho_0/\lambda_0 = 0.336$ (the break corresponds to nanowire boundary depending on the radial orientation of the dipole). The selected values of the reduced radii of the cylinders correspond to the positions of the whispering gallery modes, TM3, TE3, TM4, and TE4. The red lines correspond to the axial orientation of the dipole, green — azimuthal, blue — radial. (Colored version of the figure is presented in electronic version of the article).
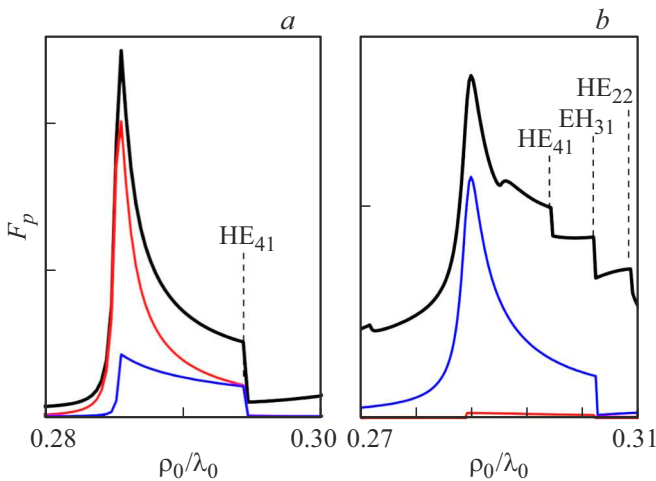
Figure 4. Purcell coefficients are given for emitter located on the outer boundary of nanowire oriented axially (*a*) and radially (*b*). The interval of reduced radii was chosen near the resonances associated with the whispering gallery modes TM4 (*a*) and TE3 (*b*). The black lines show the total values of the Purcell coefficients for the leaking modes; the contributions due to the HE_m and EH_m components (where *m* is the azimuth number) are shown by red and blue lines, respectively. The vertical dashed lines show the values of the reduced radii corresponding to the cutoffs of the waveguide modes.

increases by an order of magnitude, which is important for the use of nanowires as optical sensors.

Fig. 2, *b* and *c* show breaks in the dependences of the Purcell coefficient. Fig. 4 shows the dependences of Purcell coefficients near the resonances corresponding to WGMs.

It can be seen that these breaks are related to the cutoff frequencies of the waveguide modes: when a waveguide mode appears, the probability of emission into leaking modes decreases. The total probability of spontaneous emission in accordance with formula (20) is determined by summation over the field components characterized by all possible azimuthal numbers *m*. In this case, as shown in Fig. 4, the cutoffs of the waveguide modes make the dominant contribution to spontaneous emission near the WGMs.

Further Purcell coefficients are given for emitter located on the outer boundary of nanowire oriented axially (*a*) and radially (*b*). The interval of reduced radii was chosen near the resonances associated with the whispering gallery modes TM4 (*a*) and TE3 (*b*). The black lines show the total values of the Purcell coefficients for the leaking modes; the contributions due to the HE_m and EH_m components (where *m* is the azimuth number) are shown by red and blue lines, respectively. The vertical dashed lines show the values of the reduced radii corresponding to the cutoffs of the waveguide modes.

Promising directions for the nanowires use is the creation of sources of single photons and optical sensors based on them. In both cases, an extremely important characteristic of the emission process is not only the emission probability, but also the emission pattern. Fig. 5 shows emission patterns averaged over angle ϕ, corresponding to the peaks of the Purcell coefficient shown in Fig. 2, *b*, *c*: $\rho_0/\lambda_0 = 0.0748$ (Fig. 5, *a*, peak F_p corresponding to WGM TE0 mode); $\rho_0/\lambda_0 = 0.1678$ (Fig. 5, *b*, WGM TM2, TE1); $\rho_0/\lambda_0 = 0.2799$ (Fig. 5, *c*, WGM TE4) and $\rho_0/\lambda_0 = 0.2855$ (Fig. 5, *d*, WGM TM3). Note that the emitter is located on the surface of the nanowire (at the
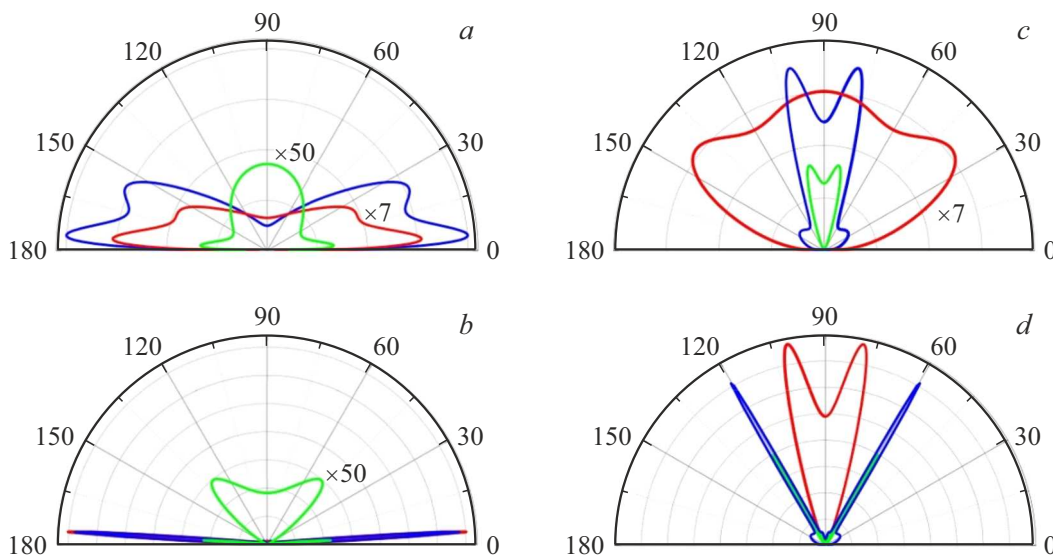
Figure 5. Emission patterns of the emitter located on the outer boundary of the nanowire, averaged over the angle ϕ, for different values of the reduced radius of the nanowire: $\rho_0/\lambda_0 = 0.0748$ (*a*); $\rho_0/\lambda_0 = 0.1678$ (*b*); $\rho_0/\lambda_0 = 0.2799$ (*c*); and $\rho_0/\lambda_0 = 0.2855$ (*d*). The selected values of the radii correspond to the maxima of the Purcell coefficient in Fig. 2, *b*, *c*. The red lines correspond to the axial orientation of the dipole, green — azimuthal, blue — radial.

point $\phi = 0$), so that the system, strictly speaking, does not have cylindrical symmetry.

It can be seen that at certain values of the reduced radius the narrow lobes of the emission pattern are formed. For $\rho_0/\lambda_0 = 0.0784$ for the radial orientation of the dipole, the emission is concentrated in a narrow range of angles near the nanowire axis. For $\rho_0/\lambda_0 = 0.167$, the concentration of emission takes place in a narrow cone with an angle θ about $5°$.

4. Conclusion

Algebraic expressions are obtained for calculating the probability of spontaneous emission for arbitrarily oriented emitter located near the nanowire or inside it. The probabilities of spontaneous emission are calculated depending on the position of the emitter and the nanowire radius. Directional patterns are calculated for various dipole orientations, and it is demonstrated that, at certain values of the reduced radius, a narrow directional pattern can be formed.

Funding

Conflict of interest

The authors declare that they have no conflict of interest.

References

[1] Katsuhiro Tomioka, Junichi Motohisa, Shinjiroh Hara, Kenji Hiruma, Takashi Fukui. Nano Lett., **10** (5), 1639 (2010).

[2] Xing Dai, Agnes Messanvi, Hezhi Zhang, Christophe Durand, Joël Eymery, Catherine Bougerol, François H. Julien, Maria Tchernycheva. Nano Lett., **15** (10), 6958 (2015).

[3] Niranjan S. Ramgir, Yang Yang, Margit Zacharias. Nanowire-based sensors, **6** (16), 1705 (2010).

[4] Haiqing Liu, Jun Kameoka, D.A. Czaplewski, H.G. Craighead. Nano Lett., **4** (4), 671 (2004).

[5] V.N. Kats, V.P. Kochereshko, A.V. Platonov, T.V. Chizhova, G.E. Cirlin, A.D. Bouravleuv, Y.B. Samsonenko, I.P. Soshnikov, E.V. Ubyivovk, J. Bleuse. Semicond. Sci. Technol., **27**, 015009 (2011).

[6] L. Leanrdo, J. Hastrup, R. Reznik, G. Cirlin, N. Akopian. NPJ Quant. Inf., **6**, 93 (2020).

[7] L. Leandro, C.P. Gunnarsson, R. Reznik, K.D. Jöns, I.V. Shtrom, A.I. Khrebtov, T. Kasama, V. Zwiller, G.E. Cirlin, N. Akopian. Nano Lett., **18**, 7217 (2018).

[8] V.G. Dubrovskii, I.V. Shtrom, R.R. Reznik, Yu.B. Samsonenko, A.I. Khrebtov, I.P. Soshnikov, S. Rouvimov, N. Akopian, T. Kasama, G.E. Cirlin. Cryst. Growth Des., **16** (12), 7251 (2016).

[9] A.C. Bleszynski, Floris A. Zwanenburg, R.M. Westervelt, Aarnoud L. Roest, E.P.A.M. Bakkers, Leo P. Kouwenhoven. Nano Lett., **7** (9), 2559 (2007).

[10] G.E. Cirlin, V.G. Dubrovskii, Yu.B. Samsonenko, A.D. Bouravleuv, K. Durose, Y.Y. Proskuryakov, Budhikar Mendes, L. Bowen, M.A. Kaliteevski, R.A. Abram, Dagou Zeze. Phys. Rev. B, **82**, 035302 (2010).

[11] E.M. Purcell. Phys. Rev., **69** (11), 681 (1946).

[12] F. Bloch. Phys. Rev., **70**, 460 (1946).

[13] J. Bleuse, J. Claudon, M. Creasey, N.S. Malik, J.-M. Gérard, I. Maksymov, J.-P. Hugonin, Lalanne, P. Inhibition. Phys. Rev. Lett., **10**, 10360 (2011).

[14] David Dzsotjan, A.S. Sorensen, M. Fleischhauer. Phys. Rev. B, **82**, 075427 (2010).

[15] T. Weiss, M. Schäferling, H. Giessen, N.A. Gippius, S.G. Tikhodeev, W. Langbein, E.A. Muljarov. Phys. Rev. B, **96**, 045129 (2017).

[16] Y. Chen, T.R. Nielsen, N. Gregersen, P. Lodahl, J. Mork. Phys. Rev. B, **81**, 125431 (2010).

[17] J. Bleuse, J. Claudon, M.Creasey, N.S. Malik, J.-M. Gérard, I. Maksymov, J.-P. Hugonin, P. Lalanne. Phys. Rev. Lett., **106**, 10360 (2011).

[18] R.R. Reznik, G.E. Cirlin, K.P. Kotlyar, I.V. Ilkiv, N. Akopian, L. Leandro, V.V. Nikolaev, A.V. Belonovski, M.A. Kaliteevski. Nanomaterials, **11**, 2894 (2021).

[19] R. Paniagua-Domínguez, G. Grzela, J.G. Rivas, J.A. Sánchez-Gil. Nanoscale, **5** (21), 10582 (2013).

[20] Diego R. Abujetas, Ramón Paniagua-Domínguez, José A. Sánchez-Gil. ACS Photonics, **2** (7), 921 (2015).

[21] Dick van Dam, Diego R. Abujetas, Ramón Paniagua-Domínguez, José A. Sánchez-Gil, Erik P.A. M.Bakkers, Jos E.M. Haverkort, Jaime Gómez Rivas. Nano Lett., **15** (7), 4557 (2015).

[22] C.F. Bohren, D.R. Huffman. *Absorption and Scattering of Light by Small Particles* (Wiley, N.Y., 1998).

[23] M.A. Kaliteevski, S. Brand, R.A. Abram, A. Kavokin, Le Si Dang. Phys. Rev. B, **75**, 233309 (2007).